JOURNAL OF CATALYSIS 142, 672–690 (1993)

# Structure and Distribution of Alkali Promoter in $K/MoS_2$ Catalysts and Their Effects on Alcohol Synthesis from Syngas

HEE CHUL WOO,[1] IN-SIK NAM,[2] JAE SUNG LEE, JONG SHIK CHUNG, AND YOUNG GUL KIM

*Research Center for Catalytic Technology, Pohang Institute of Science and Technology (POSTECH) and Research Institute of Industrial Science and Technology (RIST), P.O. Box 125, Pohang, 790-600, Korea*

Received November 20, 1992; revised April 5, 1993

Potassium-promoted $MoS_2$ catalysts were investigated by scanning Auger electron spectroscopy, electron probe microanalysis, X-ray energy dispersive spectroscopy, and elementary chemical analysis to elucidate the role of potassium on $MoS_2$. Fresh samples exhibited a uniform distribution of the alkali elements by CO hydrogenation, whereas the oxidized sample showed a segregation of the potassium component in the bulk of the catalyst. The fresh $K_2CO_3$-, $K_2O_2$-, and $K_2S$-promoted $MoS_2$ catalysts show high selectivities to alcohols and their IR spectra present two characteristic bands at 1650 and 1400 $cm^{-1}$ assigned to a bicarbonate-like species which is believed to be an active intermediate for the synthesis of alcohols. No such IR bands appear in the cases of $K_2SO_4$- and KCl-promoted $MoS_2$ and oxidized $K_2CO_3/MoS_2$ catalysts which mainly produce hydrocarbons instead of alcohols. A mechanism based on this intermediate is proposed for the alcohol formation from $CO-H_2$. In addition, the enhanced catalytic activity and high selectivity to $C_{2+}$ hydrocarbons of the oxidized $K_2CO_3/MoS_2$ is believed to be due to the transfer of electron from the alkali metal diffused into the bulk of $MoS_2$, resulting in an increase in electron density as well as in the density of states at the Fermi surface. The alkali metal on the $MoS_2$ acts as a medium for oxygen supply ("sponge") in the atmosphere and promotes oxidation of Mo(IV) to Mo(VI) and $S^{2-}$ to $S^{6+}$ states. 

## INTRODUCTION

Transition-metal-sulfide-based catalysts have been widely used for more than a half century in hydrodesulfurization, hydrodenitrogenation, and hydrogenation reactions which occur during petroleum hydroprocessing and hydrofinishing. Recently, there has been a growing interest for the catalytic activity of $MoS_2$ catalyst on the synthesis of alcohols from CO and $H_2$ (*1–3*). The sulfide based catalysts are able to maintain high activity even in the presence of considerable amounts of sulfur in the feed. Furthermore, they are very good water–gas shift catalysts, and hence could perform well with low $H_2/CO$ feed ratios of syngas (*4*). In the hydrogenation of carbon monoxide over $MoS_2$ catalysts for mixed alcohol synthesis, it is essential that a certain amount of potassium salt should be present on the catalyst. Addition of potassium to the $MoS_2$ has a significant impact on the catalytic activity: CO conversion is lowered, and the primary products shift from alkanes to alcohols (*5–8*). Note that alkali metals are commonly used as promoters for many catalytic reactions such as Fischer–Tropsch synthesis (*9, 10*), ammonia synthesis (*1*), and mixed alcohol synthesis (*6, 12–14*).

The role of promoters is generally classified as either structural and/or chemical (or electronic) depending on their primary function. Structural promoters are added to create a high and stable surface area of the catalyst, whereas chemical promoters improve the catalytic performance of catalyst. In particular, the effect of the alkali metal on a given catalyst can manifest itself in

[1] Present address: Department of Chemical Engineering, Pusan National University of Technology, Pusan 608-739, Korea.

[2] To whom correspondence should be addressed.



0021-9517/93 $5.00

two ways, e.g., (i) improvement in selectivity and/or activity and (ii) extension of catalyst lifetime (*15*).

Recently, the modification of surface structure and catalytic behavior of $K_2CO_3/MoS_2$ catalyst was investigated by its exposure to atmosphere for an extended period of time after preparation (*16*). The oxidized $K_2CO_3/MoS_2$ catalyst showed enhanced catalytic activity and high selectivity for $C_{2+}$ hydrocarbons, rather than forming alcohols as did on fresh $K_2CO_3/MoS_2$. In this regard, $K_2CO_3/MoS_2$ may be a interesting catalytic system to study how both alcohol and hydrocarbon synthesis are influenced by the presence of an alkali promoter on the surface of catalyst.

The present study extends the previous work (*16*) on the surface properties of the $K_2CO_3/MoS_2$ catalyst. In addition to infrared spectroscopy (IR) used before, the techniques of scanning electron microscopy (SEM) and scanning Auger electron spectroscopy (SAES) were used to examine the topography as well as the laterally resolved composition of the catalyst surface. Electron probe microanalysis (EPMA) and energy dispersive X-ray spectroscopy (EDS) were also used to determine the distribution of promoters. The characteristics of the catalysts were correlated with their catalytic performance for the formation of mixed alcohols. Fresh $K_2CO_3/MoS_2$ catalyst was also compared with the one aged in atmosphere.

## EXPERIMENTAL

### *Catalyst Preparation*

The catalysts were prepared by methods similar to those outlined by Dianis (*17*). Briefly, $MoS_2$ was prepared by the thermal decomposition of $(NH_4)_2MoS_4$ in flowing helium at 773K for two hours. The $MoS_2$ was ground together with 17 wt% $K_2CO_3$ in a glass mortar to obtain the fresh catalyst (K/Mo = 0.5). The oxidized catalyst was also prepared by exposing the fresh catalyst to the atmosphere during the period of 13 weeks. Results of XPS and IR analysis of oxidized catalysts showed characteristics identical to those observed in the previous work (*16*), such as the oxidations of Mo(IV) to Mo(VI) as well as $S^{2-}$ (sulfide) to $S^{6+}$ (sulfate). The $K_2O_2$-, $K_2S$-, KCl-, and $K_2SO_4$-promoted $MoS_2$ (K/Mo = 0.5) were also prepared by the same method for $K_2CO_3/MoS_2$ catalyst to study the role of K on $MoS_2$.

### *Methods of Characterization*

The characterization of physicochemical properties of a heterogeneous catalyst that is to be correlated to their catalytic activity requires several techniques. The characterization methods of the catalyst employed in this study are SAES for surface chemistry and composition, EDS/EPMA for bulk composition and distribution, SEM for morphology, and XRD for bulk structure.

The techniques of scanning electron microscopy (SEM, Philips SEM 515) and scanning Auger electron spectroscopy (SAES, PHI 590 SAM system, lateral resolution about 1000 Å) were used for the characterization of the catalyst topography as well as a laterally resolved composition of the surface. It should be noted that the "Auger maps" could be correlated with corresponding features in the surface topography. The quantitative evaluation of the surface composition from SAES data was achieved by recording the peak-to-peak amplitudes of the respective elements and by using the corresponding sensitivity factors (*18*).

Energy-dispersive X-ray spectra (EDS) were obtained with an EDAX PV 9100 microanalyzer. Samples were mounted on graphite stubs and approximately 300 Å of gold was sputtered onto catalysts to ensure an adequate conductivity. Also the distribution of potassium promoter on the samples was examined by Hitachi HSM-2B electron probe microanalyzer (EPMA).

Infrared spectra were recorded with a Perkin–Elmer 1800 FT-IR double beam spectrometer on KBr pellets containing

0.5–1.0 wt% of catalyst sample powder. All spectra were determined by the averages of 16 individual scans made at room temperature with a resolution of 4.0 $cm^{-1}$.

*Catalytic Reaction*

The catalytic reaction was carried out in a tubular down flow fixed-bed reactor at $CO/H_2$ = 1.0, 573 K, 1.5 MPa, and a contact time ($W/F$) of 7.2 g-catalyst h $mol^{-1}$. Nitrogen served as an internal standard for the calculation of activity. Procedures to test catalyst performance has been described in detail elsewhere (*19*).

## RESULTS

*Surface Characterization*

The scanning electron micrographs (SEM) of fresh and oxidized catalysts before and after reaction are shown in Figs. 1a–4a with a low magnification. The morphological differences among these samples are not evident yet. The catalyst samples, however, show irregular shapes with different sizes, and contain considerable amount of agglomerates and plate-like crystallites. Superficially, the effect of alkali addition to the catalysts dose not appear in all samples. The lateral distributions of the elements Mo, S, and K over the same region of the catalyst sample as examined by SEM (Figs. 1a–4a) are shown in Figs. 1–4 (b–d) as "Auger maps". Note that the brightness is a relative measure of the local surface concentration, i.e., dark regions represent low concentration of the respective element. As expected, the fresh catalyst prepared by mechanical mixing of $MoS_2$ and potassium carbonate contains little K on the catalyst

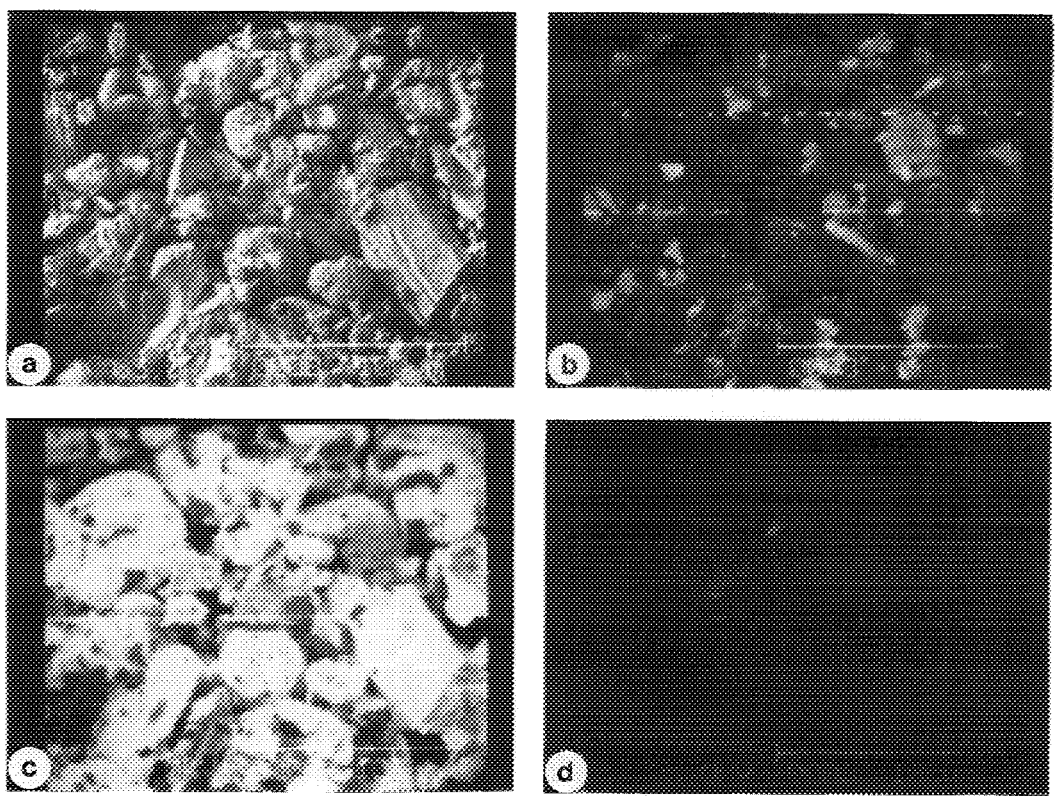


FIG. 1. "Auger maps" illustrating the lateral distributions of the elements Mo (b), S (c), and K (d) over the area of corresponding SEM image (a) for the fresh $K_2CO_3/MoS_2$ catalyst before reaction.

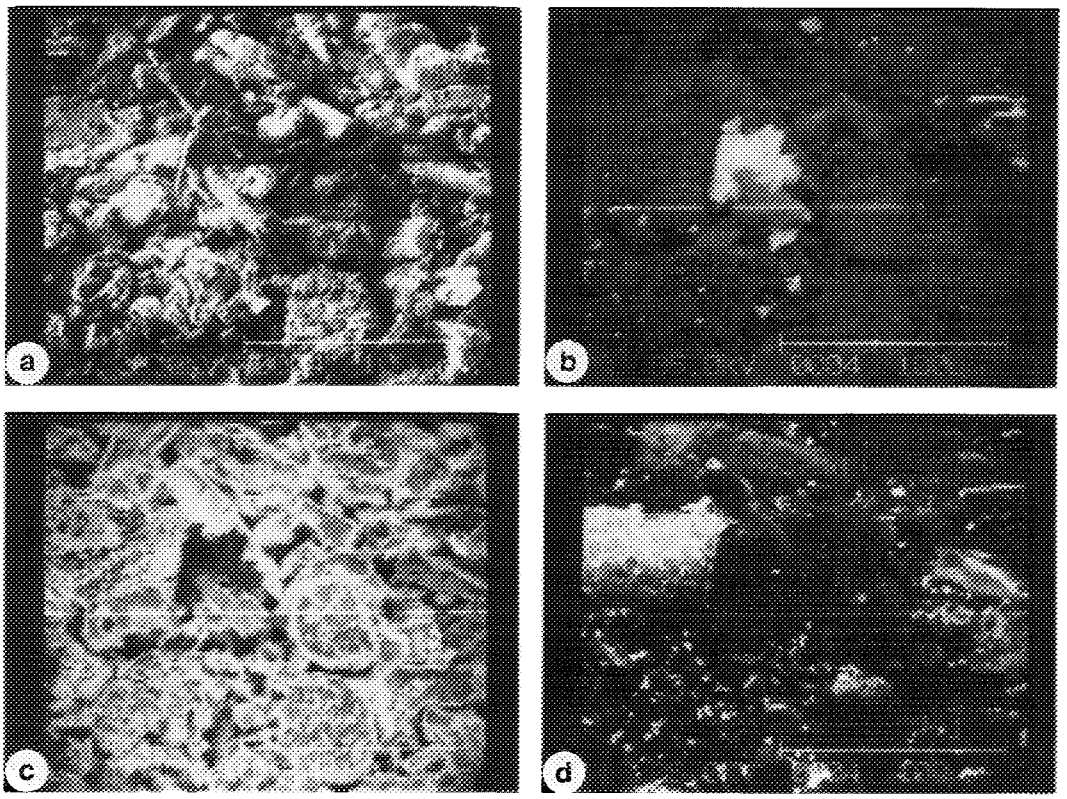


FIG. 2. "Auger maps" illustrating the lateral distributions of the elements Mo (b), S (c), and K (d) over the area of corresponding SEM image (a) for the fresh $K_2CO_3/MoS_2$ catalyst after reaction.

surface (Fig. 1d). After the reaction of CO hydrogenation the Auger map for K in Fig. 2d reveals that potassium now covers the $MoS_2$ particles more uniformly than before the reaction.

For the oxidized catalysts (Figs. 3 and 4), little difference is noticed before and after reaction. These maps represents that the surface of $MoS_2$ contains relatively little K for both cases. To illustrate the inhomogeneous lateral distribution of various elements, a series of typical Auger spectra examined for two catalysts are reproduced in Fig. 5. The fresh catalyst (Spectrum a) showed Auger peaks only due to Mo and S. After reaction (Spectrum b), K peak emerges and Mo peaks are reduced in their intensities. It indicates that the K, not observed before reaction, now appears and covers some of Mo atoms on the catalyst surface. Specta c and d of Fig. 5 obtained from oxidized catalysts show that some oxygen and a little potassium are present. Essentially no carbon signal was found with the Auger spectra, and hence $K_2CO_3$ most probably had decomposed into $K_2O$ and $CO_2$ under the influence of the electron beam during Auger experiment.

Table 1 compares these near-surface composition obtained from AES (probing depths of about 20–40 Å) with those obtained from EDS (probing depths of a few micrometers) and chemical analysis (bulk composition). The general trend listed in Table 1 for the fresh and oxidized $MoS_2$ catalysts is the increase in the relative concentration of K examined by the above techniques with increasing probing depth. The

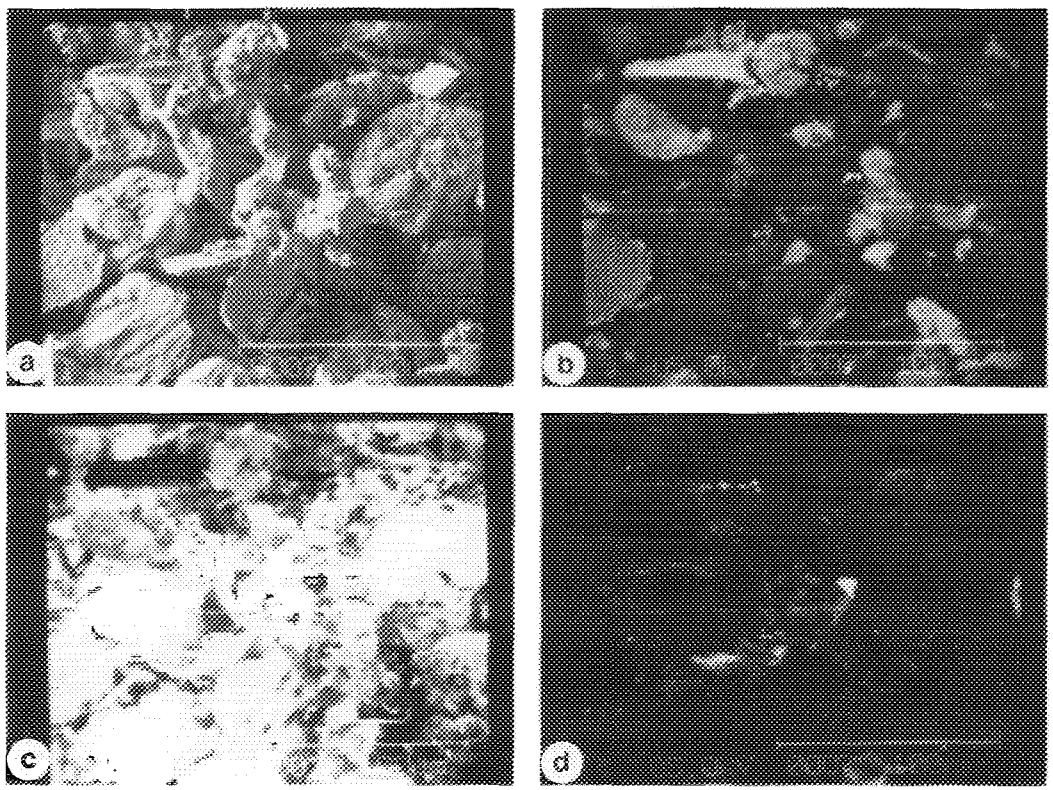

FIG. 3. "Auger maps" illustrating the lateral distributions of the elements Mo (b), S (c), and K (d) over the area of corresponding SEM image (a) for the oxidized $K_2CO_3/MoS_2$ catalyst before reaction.

TABLE 1

Relative Weight Concentrations of the Mo, S, and K Components in Fresh and Oxidized $K_2CO_3/MoS_2$ Catalysts as Determined by Chemical Analysis (CA), EDS, and AES

| | Fresh catalyst | | | Oxidized catalyst | | |
|---|---|---|---|---|---|---|
| | Mo | S | K | Mo | S | K |
| | Before reaction | | | | | |
| AES | 52.3 | 47.5 | 0.2 | 51.1 | 48.4 | 0.5 |
| EDS | 46.1 | 44.7 | 9.2 | 50.7 | 42.6 | 6.7 |
| CA | 49.3 | 38.0 | 12.7 | 50.4 | 35.3 | 14.3 |
| | After reaction | | | | | |
| AES | 44.7 | 49.1 | 6.2 | 54.2 | 44.5 | 1.3 |
| EDS | 42.8 | 46.7 | 10.5 | 57.0 | 39.6 | 3.4 |
| CA | 50.5 | 36.7 | 12.8 | 50.5 | 36.8 | 12.7 |

*Note.* All concentrations are normalized to 100% excluding oxygen and carbon.

most significant difference between these catalysts lies in the marked surface enrichment of K in the fresh $K_2CO_3/MoS_2$ catalyst after the reaction of CO hydrogenation, thus revealing that this element is dispersed on the $MoS_2$ surface during the course of reaction. The oxidized catalyst samples indicate that most of the K remains in subsurface regions both before and after the reaction.

### *Bulk Characterization*

X-ray energy dispersive spectroscopy (EDS) and electron probe microanalysis (EPMA) were used to provide further information for the concentration profiles of alkali promoters on the catalyst surface (*15, 20, 21*). Both techniques use a focused beam of electrons to excite characteristic

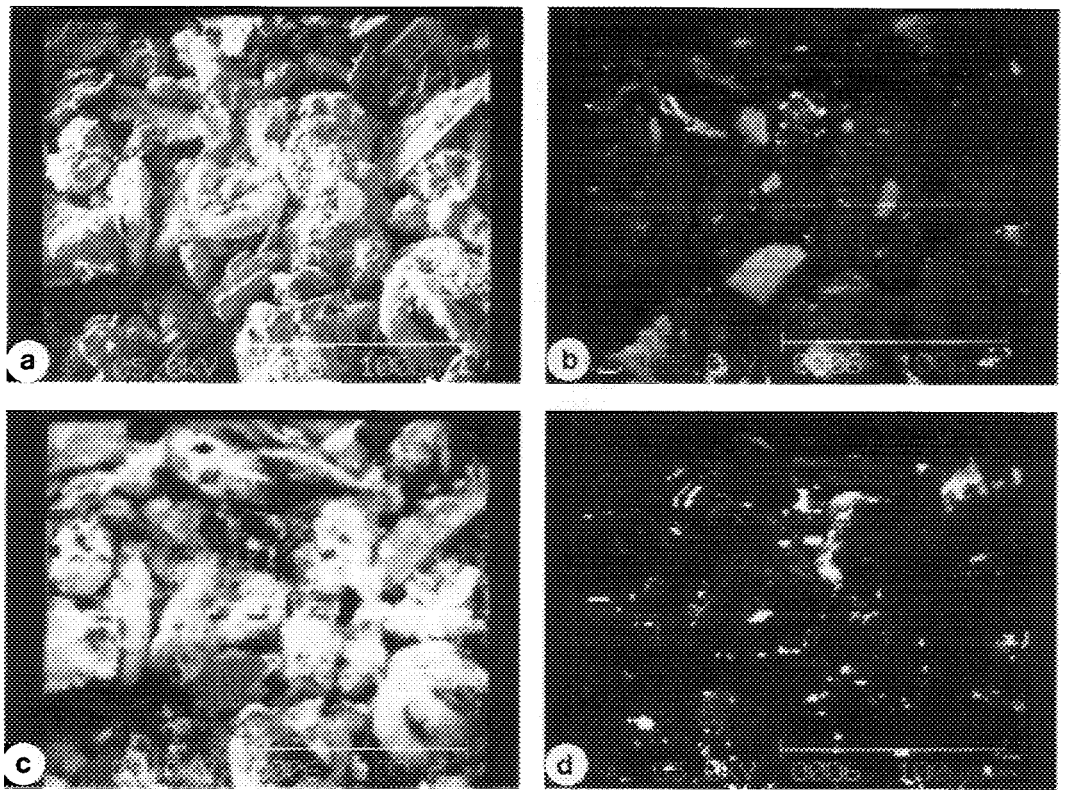


FIG. 4. "Auger maps" illustrating the lateral distributions of the elements Mo (b), S (c), and K (d) over the area of corresponding SEM image (a) for the oxidized $K_2CO_3/MoS_2$ catalyst after reaction.

X-rays within the top 1–4 $\mu$m layer of the sample, and therefore the indicated compositions may refer to the concentrations of bulk region. Typical X-ray spectra ("X-ray map") with corresponding SEM micrographs are shown in Figs. 6, 8, 10, and 12. Scans of each element along the central horizontal line of the micrographs are presented in Figs. 7, 9, 11, and 13. The inhomogeneity of K distribution on the catalyst surface was observed for the fresh $K_2CO_3/MoS_2$ before CO hydrogenation, while a uniform dispersion was observed after the reaction. For the oxidized $K_2CO_3/MoS_2$ the corresponding potassium X-ray map showed more inhomogeneous dispersion of K with some agglomeration both before and after the reaction.

*Catalytic Reaction and IR Measurements*

In order to obtain better understanding of the chemical nature of potassium under the reaction conditions of syngas, the various potassium salts having different thermal stability and electron affinity were added to $MoS_2$. Potassium sulfide ($K_2S$), potassium peroxide ($K_2O_2$), potassium carbonate ($K_2CO_3$), potassium chloride (KCl), and potassium sulfate ($K_2SO_4$) were employed as alkali promoters for this study. The $K_2O_2$ were prepared by the thermal decomposition of superoxide ($KO_2$) in flowing helium at 673 K (*22*).

The alkali promoter may be added to $MoS_2$ by either physical mixing or solution impregnation (*1*, *2*). In our previous works

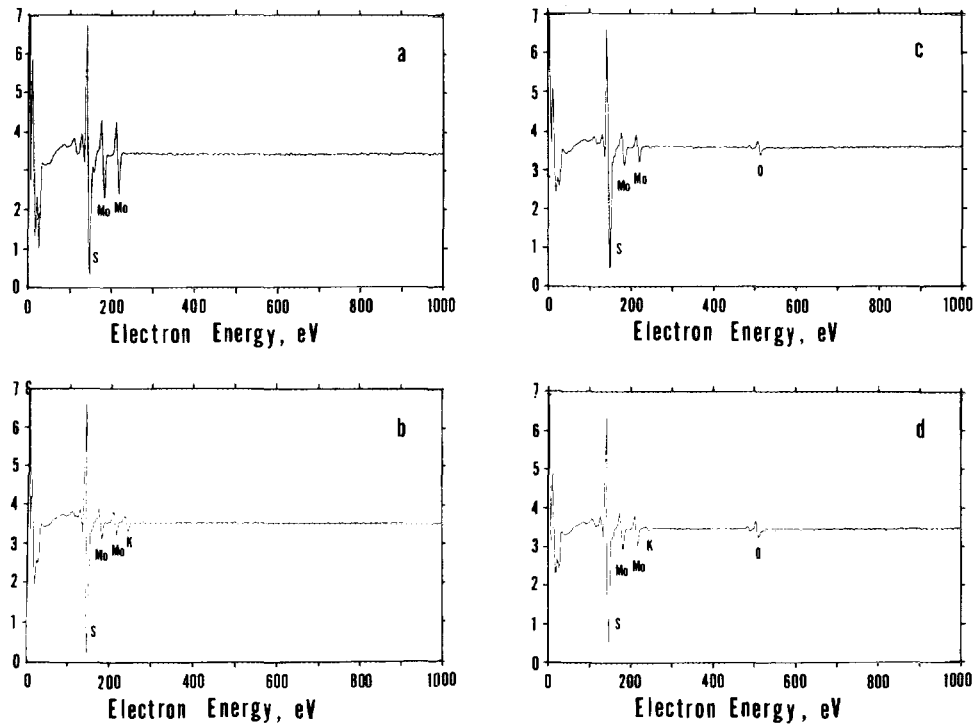


FIG. 5. Typical Auger electron spectra observed for the areas of corresponding SEM images (same areas as in Figs. 1a–4a) of the surface of fresh and oxidized catalysts before and after reaction: (a) fresh catalyst before reaction, (b) fresh catalyst after reaction, (c) oxidized catalyst before reaction, and (d) oxidized catalyst after reaction.

(*8*, *16*) both methods yielded catalysts showing the same activity and selectivity in the reaction. Catalyst performance was essentially independent of the method of alkali addition in qualitative agreement with the results of others (*5*, *6*).

Figure 14 shows the changes in the total activity and selectivity to alcohols with time on stream over various alkali-promoted catalysts. In the cases of $K_2S$-, $K_2O_2$-, and $K_2CO_3$-promoted $MoS_2$, total activity decreased monotonously, while alcohol selectivity increased drastically with the time. Although the deactivation rate was not exactly the same for all of these catalysts as shown in Fig. 14, the similar patterns for the alcohol selectivity vs the time on stream were evident. It is a typical effect of alkali promotion for mixed alcohol catalysts and the suppression of hydrogenation ability has been identified as a major effect of alkali-promoters for CO hydrogenation over transition metal catalysts (*23*). This modification of total activity and alcohol selectivity with respect to time indicates that the nature of the catalyst surface may have been significantly altered during the course of reaction. However, $K_2SO_4$- and KCl-promoted $MoS_2$ catalysts show lower selectivity for alcohol formation. It suggests that the selectivity for alcohol formation strongly depends on the counter anion of the potassium salts employed in this study. The ineffectiveness of $SO_4^{2-}$ and $Cl^-$ in the alcohol synthesis might be due to the stability of these anions as reflected in their thermal stability and strong electron affinities (*24*, *25*).

Here one must consider the possibility of hydrocarbon formation resulting from the

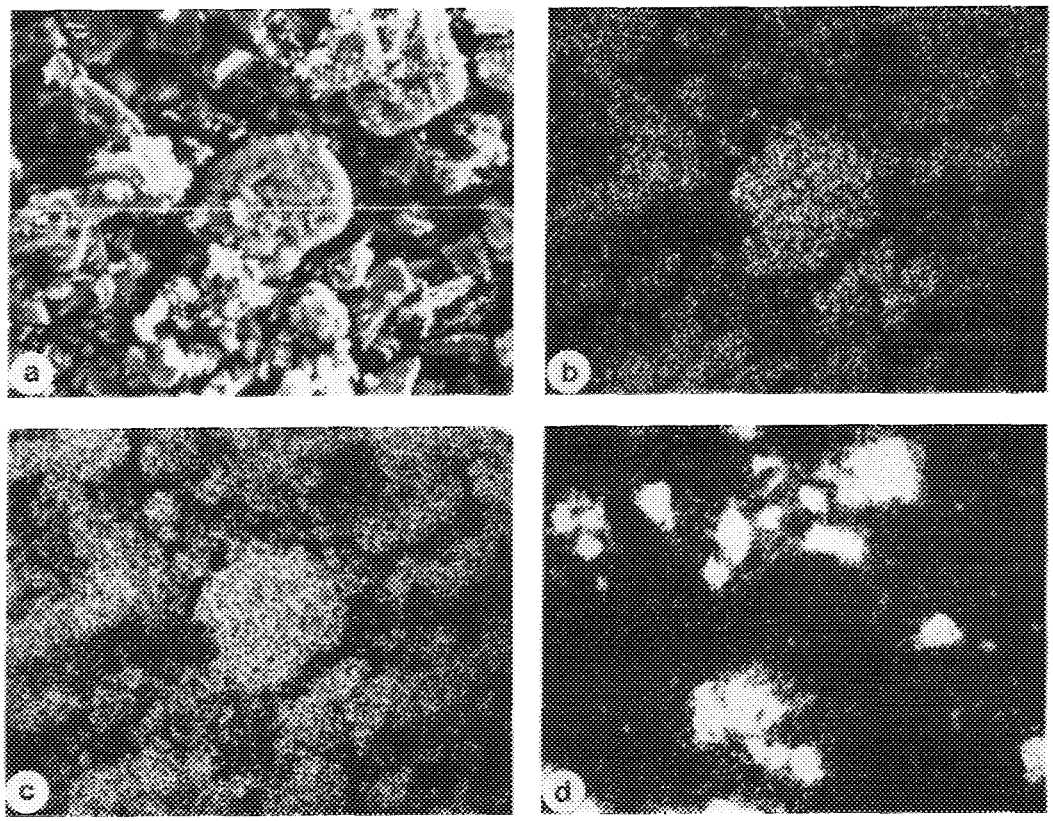


FIG. 6. Electron probe microanalysis of the fresh catalyst before reaction (magnification 500×): (a) SEM image, (b) Mo, (c) S, and (d) K.

alcohol dehydration on the acid sites. It is reported that the addition of $K_2CO_3$ largely reduces the activity by poisoning the acid sites on the catalyst, while increases the selectivity for the alcohols (*14*). In order to check this possibility, Table 2 compares the oxidized and fresh $K_2CO_3/MoS_2$ catalyst at similar CO conversions and under the same reaction conditions. The selectivity patterns of the two types of $K_2CO_3/MoS_2$ are markedly different from each other, indicating that hydrocarbon formation over oxidized $K_2CO_3/MoS_2$ is not a result of the secondary dehydration reaction of alcohol intermediates due to increased CO conversions, but an intrinsic property of the catalyst.

The chemical states of the fresh and oxidized $K_2CO_3/MoS_2$ catalysts were investigated by means of IR and XPS in the previous work (*16*). The oxidized $K_2CO_3/MoS_2$ catalysts contained sulfate species with the structure of point groups $T_d$ and $C_{2v}$, whereas the fresh $K_2CO_3/MoS_2$ had a pair of strong absorption bands at 1400 and 1653 $cm^{-1}$ which were assigned to carbonate species. The additional information for the carbonate species was obtained from the FT-IR spectra of $K_2S$-promoted $MoS_2$ catalysts in Fig. 15. Note that $K_2S$ is a compound without oxygen and carbon atoms. The IR spectra of $K_2S/MoS_2$ before and after the reaction of CO hydrogenation are shown in Fig. 15 along with the spectrum of $K_2S$. Obviously, spectrum c showed two intense bands appearing in the region of 1650

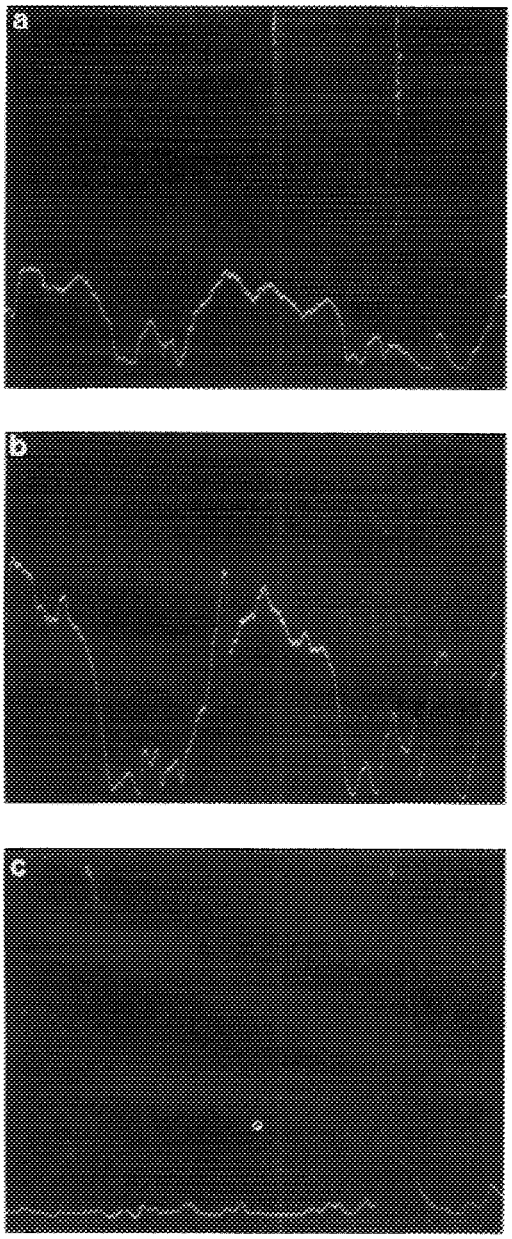

FIG. 7. Concentration profiles obtained by an electron probe microanalysis of the elements Mo (a), S (b), and K (c) (scans were made along horizontal line for the fresh catalyst before reaction).

and 1400 $cm^{-1}$ at the expense of the characteristic band related to the $K_2S$ component. These bands were also observed by Yuh and Wolf (*26*) in their FT-IR spectra of potassium catalyst for the reaction of coal chars and carbons. They found that the bands appeared at the same frequencies as those for pure $KHCO_3$ in pure, carbon impregnated, devolatilized, and partially gasified forms. These bands were assigned to the bicarbonate-like species formed by the participation of C–O–K bonds as well as C–O–H bonds. The $K_2O_2$-promoted $MoS_2$ catalysts also showed two characteristic bands at 1650 and 1400 $cm^{-1}$. Hence the two IR peaks appear to be a common feature of all active catalysts for alcohol synthesis. In contrast, no such bands appeared in the case of catalysts producing mostly hydrocarbons, such as, $K_2SO_4$- and KCl-promoted $MoS_2$ catalysts, and oxidized $K_2CO_3/MoS_2$.

## DISCUSSION

### *Fresh Potassium-Promoted $MoS_2$ as an Alcohol Selective Catalyst*

Fresh $K_2CO_3/MoS_2$ catalyst prepared by the mechanical mixing showed that the

TABLE 2

Performance of Fresh and Oxidized $K_2CO_3/MoS_2$ Catalysts[a]

| Catalyst | Fresh | Oxidized |
|---|---|---|
| CO conv. (%) | 12.6 | 15.5 |
| $CO_2$ yield (%) | 5.0 | 5.4 |
| Carbon atom selectivity (%) | | |
| $C_1$ | 21.6 | 28.2 |
| $C_{2+}$ | 7.9 | 59.6 |
| $\Sigma$(HC)[b] | (29.5) | (87.8) |
| MeOH | 32.5 | 8.6 |
| EtOH | 30.6 | 2.6 |
| $C_{3+}$ OH | 7.4 | 1.0 |
| $\Sigma$(Alc)[b] | (70.5) | (12.2) |
| $C_2+/C_1$ ratio | | |
| HC | 0.37 | 2.11 |
| Alc | 1.17 | 0.42 |

[a] Reaction conditions: 300 K, 1.5 MPa, $H_2$/CO = 1, $W/F$ = 8.0 g-cat · h/mol, and 300 min time-on-stream.

[b] Subtotal of each product component.

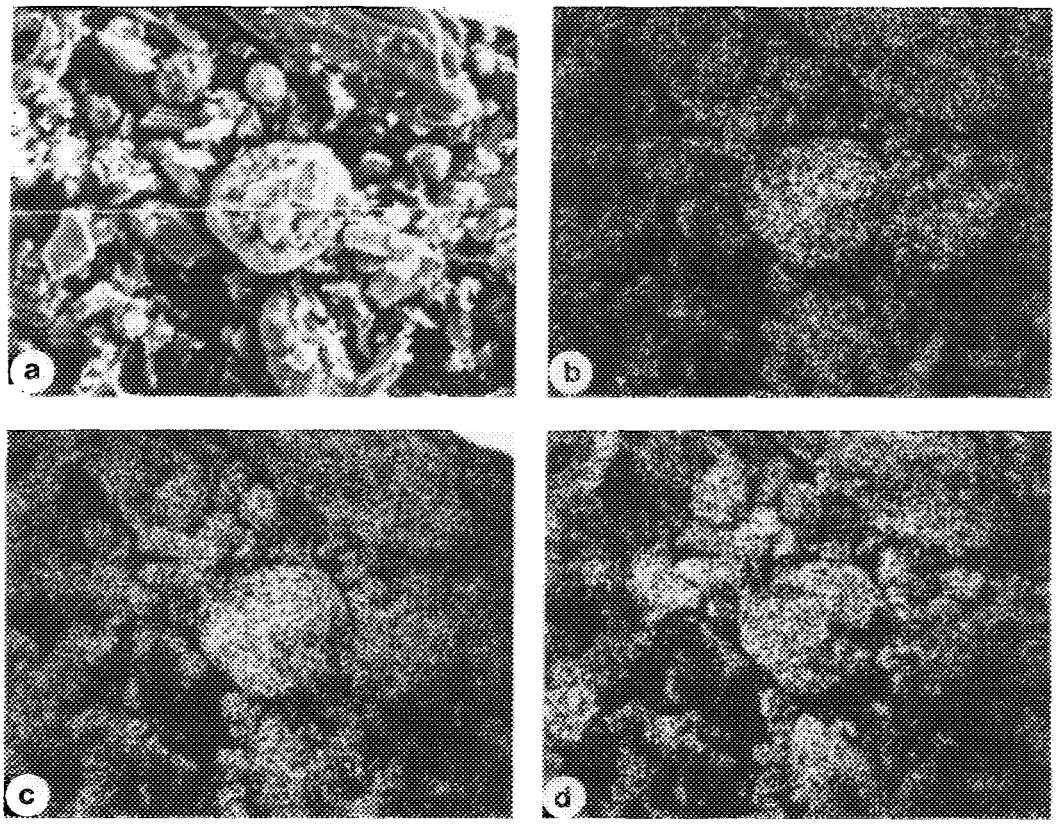


FIG. 8. Electron probe microanalysis of the fresh catalyst after reaction (magnification 500×): (a) SEM image, (b) Mo, (c) S, and (d) K.

potassium distribution is inhomogeneous (Figs. 1 and 6) as expected. After CO hydrogenation reaction, however, the catalyst achieved a fairly uniform distribution of potassium as examined by AES and EDS (Figs. 2 and 8). Due to the characteristics of these techniques, the distribution detected should be in the region near the surface. The addition of high concentration of alkali compounds to $MoS_2$ is generally known to promote the formation of alcohols. The high content of the promoter on the catalyst surface necessary to achieve the high alcohol selectivity may suggest the formation of an alkali overlayer or a surface compound on $MoS_2$ (*5*). Also, the induction period when the products change from hydrocarbons to alcohols may be the time required for the spread of alkali promoters onto the $MoS_2$ surface. The dispersion of a solid over another solid is a spontaneous process known for many other solid–solid systems (*27*). Perhaps with this amount of alkali on the surface, the weaker interaction of molecular CO with the overlayers results, and thus its direct hydrogenation dominates other reaction paths involving dissociation of CO. Then, the reaction to form alcohols might occur on the alkali overlayer not on $MoS_2$.

Kennou *et al.* (*28, 29*) have reported the change of cesium coverage on $MoS_2$. At low coverage, Cs predominantly forms ionized isolated adatoms as does on metals and

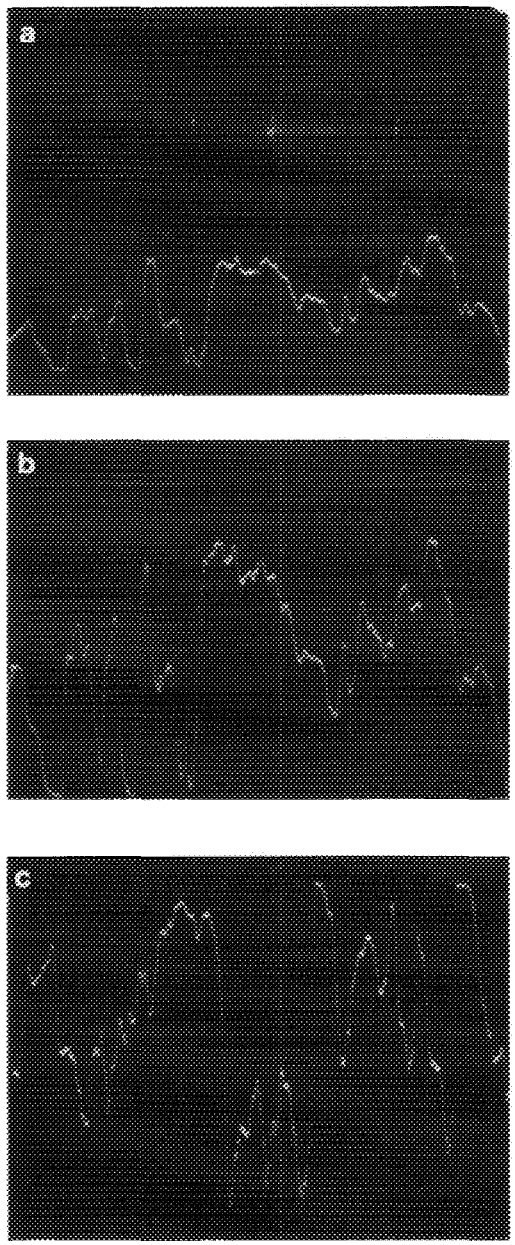


FIG. 9. Concentration profiles obtained by an electron probe microanalysis of the elements Mo (a), S (b), and K (c) (scans were made along horizontal line for the fresh catalyst after reaction).

other semiconductors. At medium and high coverage, however, Cs forms clusters on $MoS_2$ in contrast to the uniform dispersion observed on metals and other semiconductors (*28*). With such high loadings of potassium on $MoS_2$ catalyst, it is presumed that the state of potassium is either potassium clusters or a salt–surface complex. IR study indicates the presence of a salt-surface complex involving C–O–K bonds, which appears to be the active species for the alcohol formation. It is quite understandable since any known compounds of potassium including bulk $K_2O$ are not stable under the reaction conditions studied in this work. Similar salt–surface complexes have also been postulated for the copper (*20*) and iron (*30*) catalysts. This complex was not detected for KCl- and $K_2SO_4$-promoted $MoS_2$ in contrast to $K_2CO_3$-, $K_2O_2$-, and $K_2S$-promoted $MoS_2$. The ineffectiveness of catalysts containing $Cl^-$ and $SO_4^{2-}$ anions might be due to the strong electron affinity and thermal stability of these compounds; namely, they can not exist as a basic species to dope $MoS_2$. Indeed, the marked inhomogeneities of potassium distribution were detected by means of EDS for the KCl- and $K_2SO_4$-promoted $MoS_2$ after reaction (Fig. 16). It appears that the high dispersion of potassium in this alcohol selective catalysts has been resulted from the basic species produced by removing counter anions of alkali metals under the reaction conditions. The species may be highly mobile under the reaction conditions of CO hydrogenation.

The alcohol selective catalysts contain a bicarbonate-like salt–surface complex involving C–O–K and C–O–H bonds which exhibits the IR frequencies at 1400 and 1650 $cm^{-1}$ (Fig. 15c). Considering the normal molecular frequencies of terminal CO (1950–2130 $cm^{-1}$) or bridged CO (1850–1950 $cm^{-1}$), the low molecular frequencies of CO observed in this study may reveal an interaction between CO and potassium or other metal (*31*). It could be an indirect metal to K–CO interaction resulting in a bent configuration (*32*) or a direct interaction between K and CO involving overlap

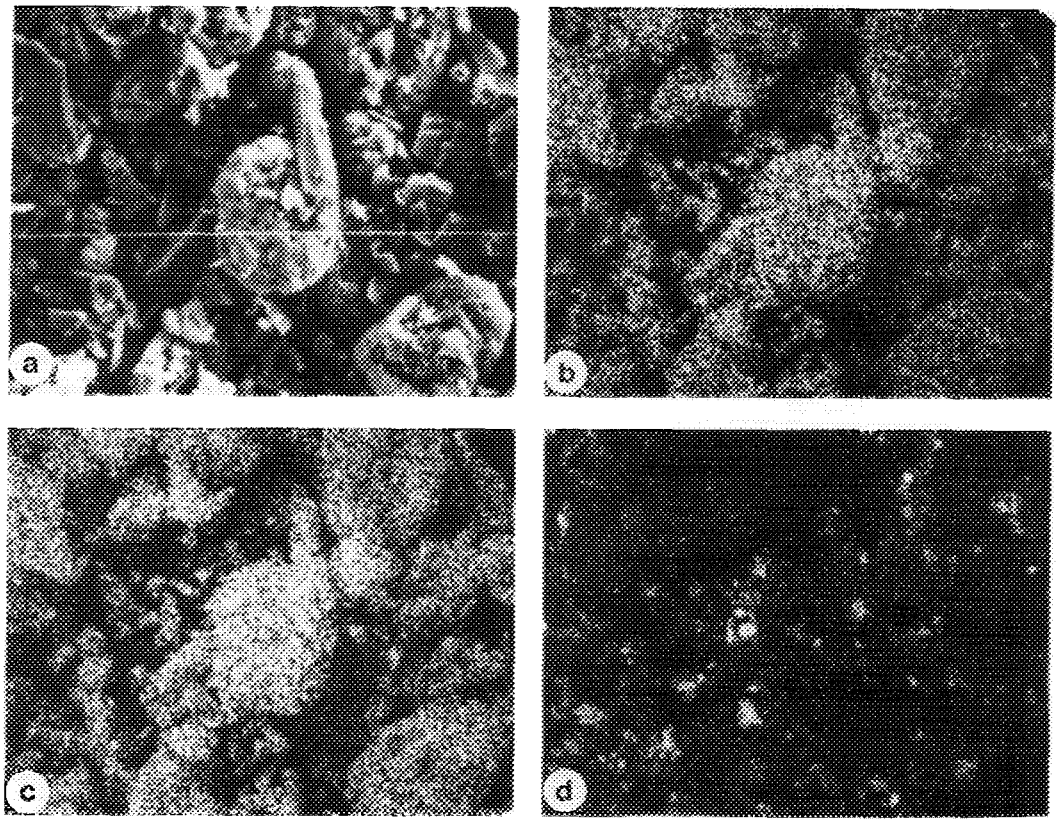


FIG. 10. Electron probe microanalysis of the oxidized catalyst before reaction (magnification 500×): (a) SEM image, (b) Mo, (c) S, and (d) K.

of the molecular orbitals as suggested by Sachtler *et al.* (*33*). Indeed, the decrease of CO in the frequencies by 300–600 $cm^{-1}$ is commonly observed in many organometallic compounds (*33*, *34*). Assuming the bent configuration of metal(M)–CO–K (*32*), a reaction scheme based on CO insertion to form alcohol compounds can be proposed:

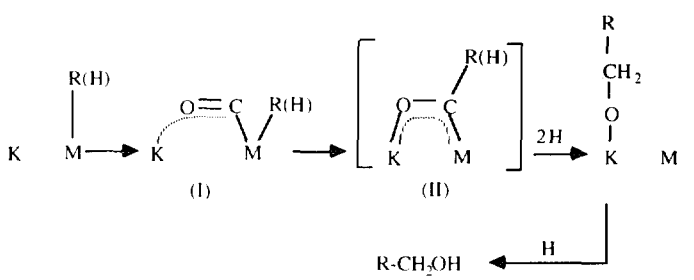


As shown, CO and H ligands will occupy coordination sites on the $MoS_2$ (M) with K bound to the oxygen of CO (I). The next step is a migratory insertion of CO and alkyl R to form an acyl intermediate (II). This step is one of the most commonly observed

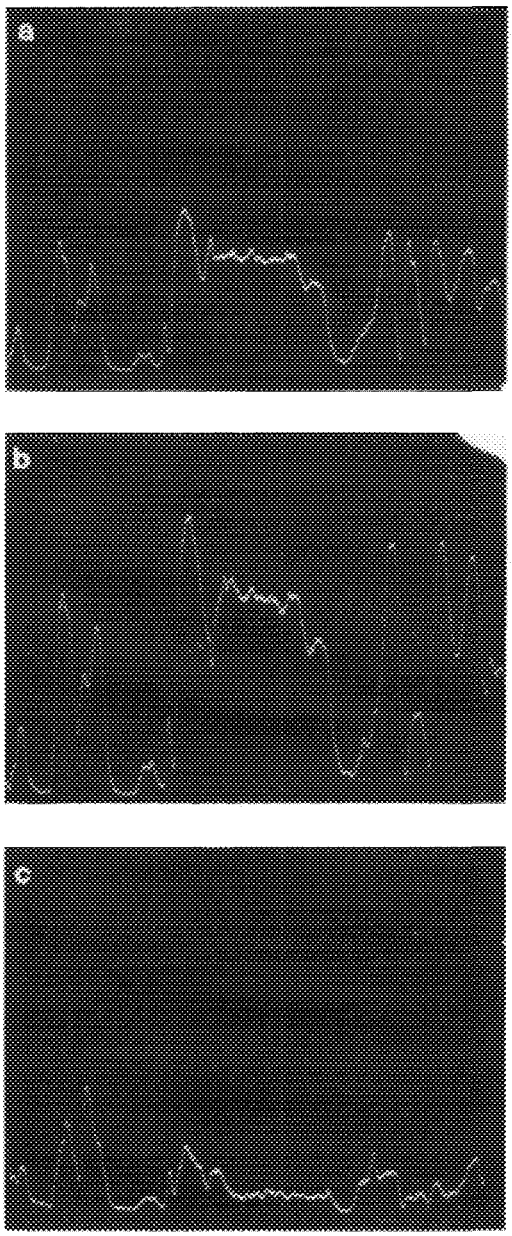

FIG. 11. Concentration profiles obtained by an electron probe microanalysis of the elements Mo (a), S (b), and K (c) (scans were made along horizontal line for the oxidized catalyst before reaction).

elementary steps in organometallic chemistry of *d*-block metals (*35*). It is believed that the coordinated CO lies in an environment of high kinetic lability under reaction conditions. The role of K here is very similar in nature to that of a Lewis acid in migratory insertion reactions on transition metal complexes. Butts *et al.* (*36*). proposed that the Lewis acid promoted these insertions (up to 50 times in rate) by binding the more basic oxygen of the acyl carbonyl group and perhaps by the stabilization of the unsaturated intermediate acyl complex. Such a role of intermediates and promoter has also been proposed by Sachtler *et al.* (*33*) in heterogeneous catalysis as well. It may provide a detailed elucidation of the proposition by Santiesteban *et al.* (*6*) that the indispensable presence of the alkali promoter is due to the bifunctionality of the catalyst, such that, the promoter activates CO and $MoS_2$ activates $H_2$.

Although there still exists a controversy whether CO insertion process is chain termination step (*23, 37*) or chain propagation step (*38*), it is generally agreed that the formation of higher alcohols requires the insertion of undissociated adsorbed CO into a $C_xH_y$ species which is generated by CO dissociation. Thus, Tacheuchi and Katzer (*39*) have suggested that higher alcohol synthesis catalysts must associate the C–O bond only at a moderate rate so that the catalyst surface contains both undissociated adsorbed CO and surface carbene species for the bimolecular insertion.

### *Oxidized Catalyst and Its Oxidation Mechanism*

The AES, EDS and chemical analysis of $K_2CO_3/MoS_2$ catalyst oxidized in the atmosphere indicate that most of K remains in the subsurface regions of the catalysts both before and after the reaction (Table 1). This highly inhomogeneous distribution of K between surface and bulk may be understood if the promoter formed large aggregates. Another possibility is that the parts of the potassium adatoms may have diffused into the subsurface regions of $MoS_2$. The catalyst showed enhanced catalytic activity and selectivity to hydrocarbons rather than to

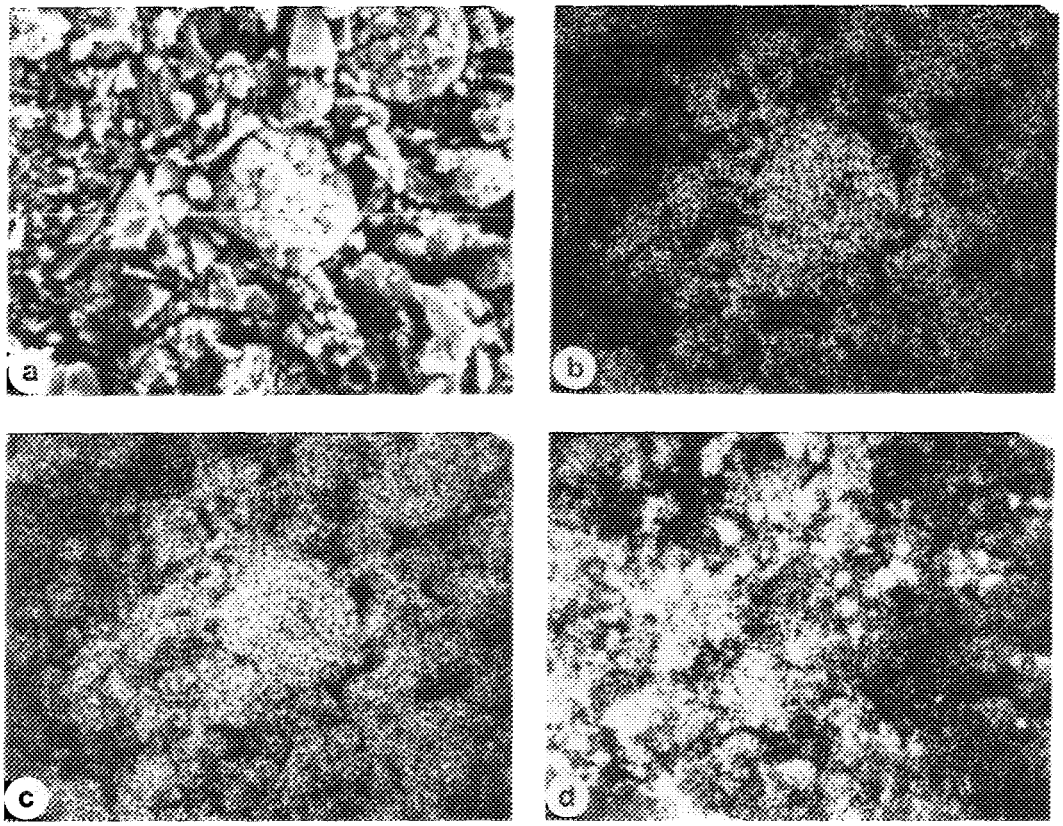


FIG. 12. Electron probe microanalysis of the oxidized catalyst after reaction (magnification 500×): (a) SEM image, (b) Mo, (c) S, and (d) K.

alcohol as observed for fresh $K_2CO_3/MoS_2$ catalyst.

In IR studies, the peaks at 1650 and 1400 $cm^{-1}$ appeared in all the active alcohol synthesis catalysts, such as, fresh $K_2CO_3$- (*16*), $K_2S$- (Fig. 15) and $K_2O_2$-promoted $MoS_2$ catalysts, but no detectable peaks were observed for the hydrocarbon synthesis catalysis such as oxidized $K_2CO_3/MoS_2$, and $K_2CO_4/MoS_2$ and $KCl/MoS_2$. Papageorgopoulos (*40*) reported that although $MoS_2$ was extremely inert to $O_2$ adsorption, the presence of Cs caused a drastic increase in the adsorption of oxygen. He also found that the parts of the Cs adatoms diffused into the subsurface regions of $MoS_2$.

Recently, there has been growing interests in the catalytic action of alkali metals on the oxidation of semiconductors (*41–43*). The alkali metal film can be deposited on the semiconducting surface prior to or simultaneously with the exposure of the surface to oxygen. These two procedures are called sequential adsorption and codeposition, respectively. In both cases the results are identical: alkali oxides appear on top of the semiconductor surface. Upon thermal annealing, massive oxidation of the substrate occurs by the transfer of the oxygen contained in these alkali oxide films to the substrate (*41*). This mechanism for thick films has been graphically termed as the "sponge" model (*41*). The alkali metal film acts as a "sponge" for oxygen, forming bulk-like compounds which transfer the oxygen to the crystal underneath upon anneal-

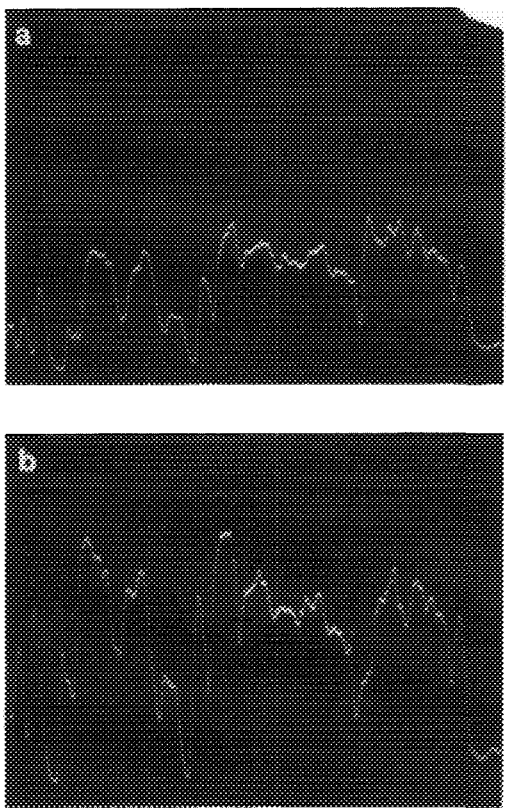


FIG. 13. Concentration profiles obtained by an electron probe microanalysis of the elements Mo (a), S (b), and K (c) (scans were made along horizontal line for the oxidized catalyst after reaction).

ing. The oxidation reaction is of course promoted by K component deposited onto the surface prior to, or simultaneously with, the oxygen exposure (*42*).

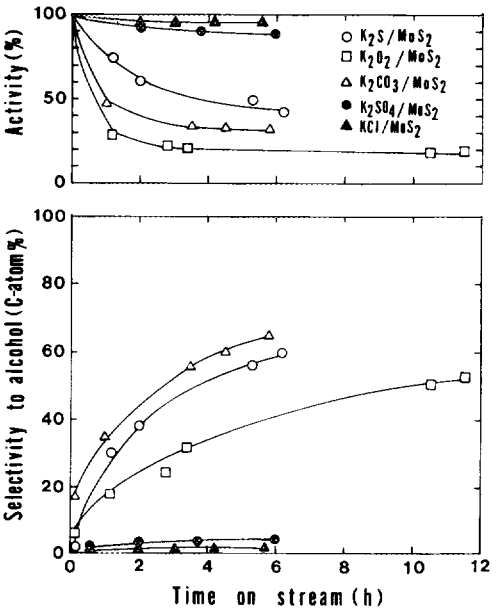


FIG. 14. Change in activity and alcohol selectivity with time on stream (activity curves were normalized for an initial activity of 100%).

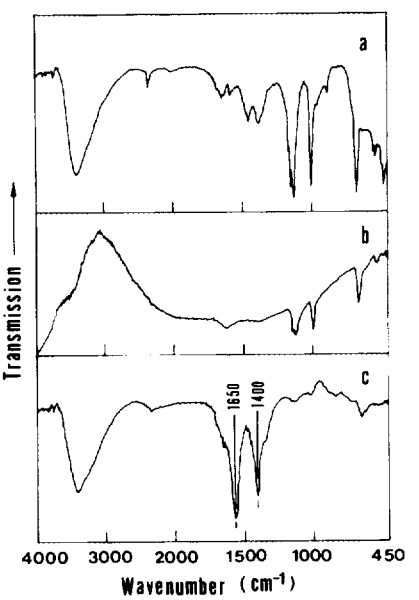


FIG. 15. IR spectra of $K_2S$-promoted $MoS_2$ catalyst: (a) $K_2S$ reference, (b) $K_2S/MoS_2$ before reaction, and (c) $K_2S/MoS_2$ after reaction.

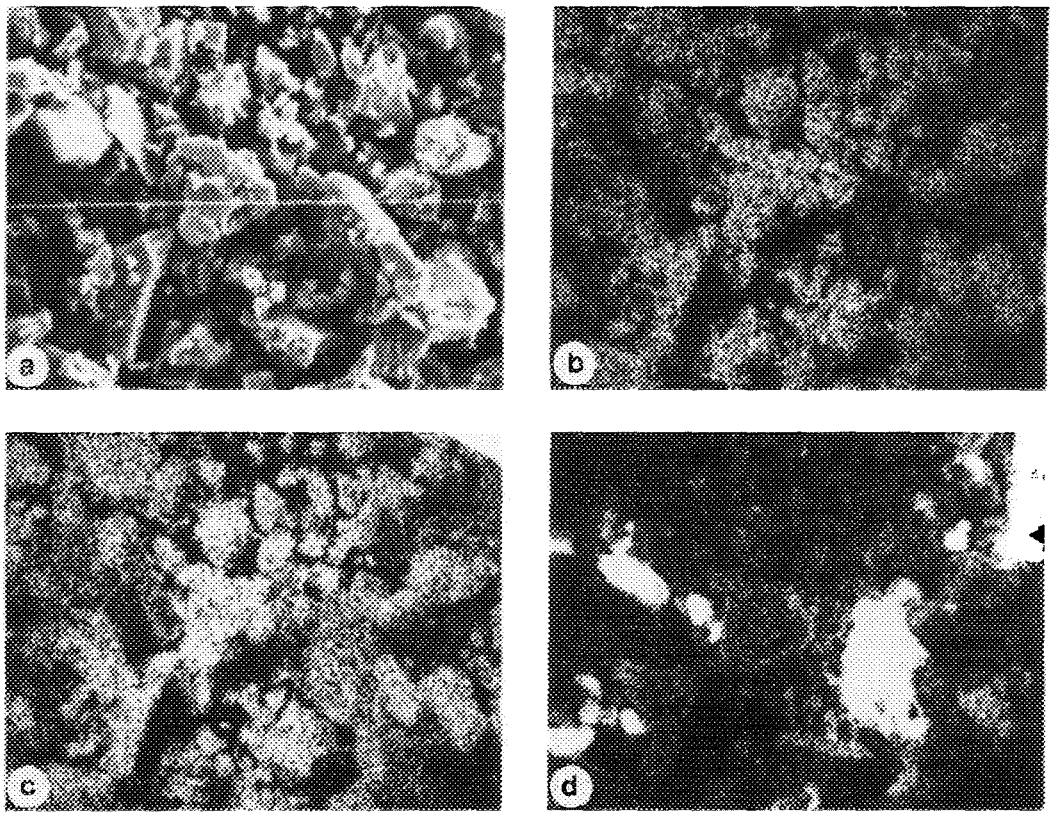


FIG. 16. Electron probe microanalysis of the $K_2SO_4/MoS_2$ catalyst after reaction (magnification 500×): (a) SEM image, (b) Mo, (c) S, and (d) K.

Soukiassian *et al.* (*43*) found an increase of the oxidation rate by a factor of $10^{13}$ in the presence of one monolayer of cesium on InP(110) surface. Karolewski and Cavell (*44*) investigated the adsorption behavior of small molecules ($O_2$, $H_2O$, HCOOH, $CO_2$, $CS_2$) on $Cs/MoS_2$ near room temperature by secondary-ion mass spectroscopy (SIMS). They found dissociative chemisorption of the molecules on $Cs/MoS_2$ with the exception of $CO_2$. Furthermore, Cs overlayers appeared to be responsible for the partial oxidation of the $MoS_2$ substrate by $O_2$ or $H_2O$.

In the previous IR and XPS studies, it has been found that the oxidized $K_2CO_3/MoS_2$ have sulfate species with $T_d$ and $C_{2v}$ symmetry as well as the Mo(VI) state (*16*). From these results and those found in the similar systems described above (*41–44*) the promoter of the oxidation appears to be K deposited onto the surface. It has also been observed that initially, physically mixed K with $MoS_2$ spreads itself onto $MoS_2$ during the oxidation when the sample was stored in the atmosphere for several weeks (Compare Fig. 6d with Fig. 10d). A mechanism responsible for the oxidation of $K_2CO_3/MoS_2$ catalyst can be schematically proposed, as depicted in Fig. 17. The potassium–oxygen compound introduced to the $MoS_2$ substrate transfers oxygen to the $MoS_2$ substrate, resulting in the oxidation of Mo(IV) to Mo(VI) and $S^{2+}$ to $S^{6+}$ states, and then K atoms diffuse into the $MoS_2$ bulk. Hence, the alkali metal introduced to

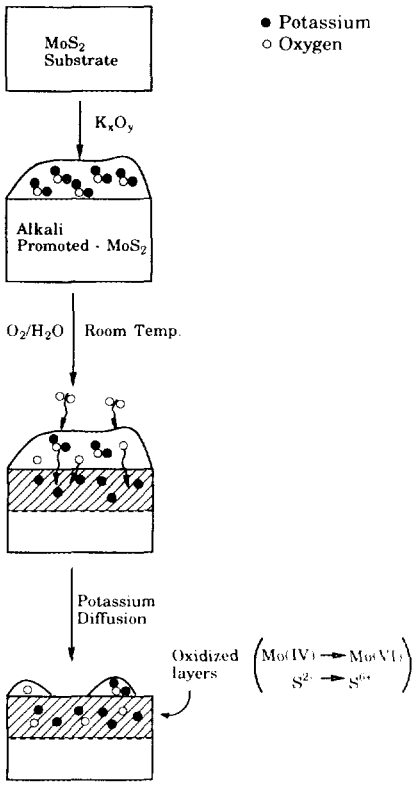


FIG. 17. Schematic diagram of a mechanism for interaction of an alkali promoter and $MoS_2$ in the atmosphere at room temperature.

the $MoS_2$ acts as "sponge" for oxygen in this process. Furthermore, the diffusion of K into bulk appears to be the cause of the autogenous dispersion of K in the oxidized sample even at room temperature. However, the exact location of the diffused K atoms in the subsurface regions of $MoS_2$ is not clear.

The formation of an intercalated bridge type compound is possible since nonstoichiometric $MoS_2$ ($Mo_{1-x}S_2$) can be formed (*45*). However, X-ray diffraction results did not show any expansion of $C_o$ axis (002 plane) due to the intercalation. The poorly crystallized nonstoichiometric $MoS_2$ such as the catalyst sample prepared by the thermal decomposition of ammonium thiomolybdate in this study is characterized by a small-coherent range of the basal plane with random stacking of the layers. In any case, it appears that a part of the K adatoms diffuse into the subsurface regions of the highly disordered $MoS_2$ and therefore, the concentration of K on the $MoS_2$ surface is reduced as shown in Table 1. This will allow an electron transfer from the alkali metal to an empty band of $MoS_2$, resulting an increase in electron density as well as the density of states at the Fermi surface. This effect may cause an increase in the metal–CO bond strength and for most cases an increase in the dissociation rate. It is apparent that the alteration of the chemical nature of the surface by alkali addition may lead different reaction paths in the overall reaction network.

The catalytic activity for the oxidized $K_2CO_3/MoS_2$ is similar to those observed over potassium modified iron foils (*46*) and nickel crystals (*47*). The oxidized $K_2CO_3/MoS_2$ catalyst showed enhanced catalytic activity and high selectivity (>95%) to $C_{2+}$ hydrocarbons (*16*). Praliaud *et al.* (*48*) have shown that potassium acts as an electronic modifier causing an electron enrichment on the metallic phase. The electron-rich metal surface will then increase the bond strength of electron-acceptor molecule CO and metal. As the adsorption strength of CO increases, hydrogen will compete less favorably to CO on the adsorption sites. From the Table 2 it is believed that the selectivity and $C_{2+}/C_1$ ratio (or carbon chain-growth) for hydrocarbons over oxidized catalyst are due to an electron donation of K diffused into the subsurface regions of $MoS_2$ rather than a secondary reaction of alcohols on the acid site. In this respect alkali metals that diffused into the oxidized catalysts is believed to be a classic electronic promoter as often observed in metal catalysts. It represents an interesting contrast to the fresh $K_2CO_3/MoS_2$, where K atoms actively participate in the reaction by providing new active sites which bind CO molecules. It is believed to be due to the fact that CO-$H_2$ reaction occurring in a reducing environment induces a homogeneous dispersion of

potassium on the $MoS_2$ surface which turns into a bicarbonate-like salt, the active species for the alcohol synthesis.

## CONCLUSIONS

Experimental study of the role of K in the K-promoted $MoS_2$ was made in the two different environments, namely, atmospheric and reductive. Experiments were performed with EDS/EPMA, Auger and IR measurements and catalytic reactions. Two environments provide the difference in the distribution of potassium on the $MoS_2$ surface and bulk. The K-promoted $MoS_2$ stored in the atmosphere for several weeks shows that K achieves an autogenous dispersion and a part of the K diffuse into the subsurface regions of $MoS_2$. In this process, alkali metal acts as a medium for oxygen supply, or "sponge." The alkali metal on the $MoS_2$ under the reductive CO hydrogenation environment disperses itself uniformly on the $MoS_2$ surface, forming a bicarbonates-like salts which is believed to be the catalytically active species for the alcohol synthesis. All alcohol-selective alkali-promoted $MoS_2$ catalyst presents two IR bands at 1650 and 1400 $cm^{-1}$ due to the bicarbonate-like species, while no such bands appear in the cases of hydrocarbon selective catalyst such as KCl- or $K_2SO_4$-promoted $MoS_2$.

## ACKNOWLEDGMENTS

The authors thank Korea Science and Engineering Foundation (KOSEF) for partial financial support through the Contract 88-0313-02. The assistance of J. K. Lee and S. H. Kim and the discussion with Dr. J. C. Kim are gratefully acknowledged.

## REFERENCES

1. Quarderer, G. J., Eur. Patent Appl. 0119609 (1984).
2. Kinkade, N. E., Eur. Patent Appl. 0149255 and 0149256 (1985).
3. Stevens, R. R., Eur. Patent Appl. 0172431 (1986).
4. Murchison, C. B., *in* "Proceedings, 4th International Conference on the Chemistry and Uses of Molybdenum" (H. F. Barry and P. C. Mitchell, Eds.), p. 197. Golden, Colorado, 1982.
5. Xie, Y., Naasz, B. M., and Somorjai, G. A., *Appl. Catal.* **27,** 233 (1986).
6. Santiesteban, J. G., Bogdan, C. E., Herman, R. G., and Klier, K., *in* "Proceedings, 9th International Congress on Catalysis, Calgary, 1988" (M. J. Phillips and M. Ternan, Eds.), Vol. 2, p. 561. Chem. Institute of Canada, Ottawa, 1988.
7. Murchison, C. B., Conway, M. M., Stevens, R. R., Quarderer, G. J., *in* "Proceedings, 9th International Congress on Catalysis, Calgary, 1988" (M. J. Phillips and M. Ternan, Eds.), Vol. 2, p. 626. Chem. Institute of Canada, Ottawa, 1988.
8. Woo, H. C., Kim, Y. G., Moon, S. H., Nam, I-S., Lee, J. S., and Chung, J. S., *Hwahak Konghak (J. Korean Inst. Chem. Eng.)* **28,** 552 (1990).
9. Dry, M. E., and Oosthuizen, G. J., *J. Catal.* **11,** 18 (1968).
10. Dry, M. E., Shingles, T., Boshoff, L. J., and Oosthuizen, G. J., *J. Catal.* **15,** 190 (1969).
11. Van Ommen, J. G., Bolink, W. J., Prasad, J., and Mars, P., *J. Catal.* **38,** 120 (1975).
12. Smith, K. J., and Anderson, R. B., *Can. J. Chem. Eng.* **61,** 40 (1983).
13. Courty, P., Durand, D., Freund, E., and Sugier, A., *J. Mol. Catal.* **17,** 241 (1982).
14. Tatsumi, T., Muramatsu, A., and Tominaga, H., *Appl. Catal.* **34,** 77 (1987).
15. Pennock, G. M., Flower, H. M., and Anderew, S. P. S., *J. Catal.* **103,** 1 (1987).
16. Woo, H. C., Nam, I-S., Lee, J. S., Chung, J. S., Lee, K. H. and Kim, Y. G., *J. Catal.* **138,** 525 (1992).
17. Dianis, W. P., *Appl. Catal.* **30,** 99 (1987).
18. Davis, L. E., MacDonald, N. C., Pamberg, P. W., Riach, G. E., and Weber, R. E., "Handbook of Auger Electron Spectroscopy." Physical Electronics Industries, Eden Prairie, Minn., 1976.
19. Woo, H. C., Park, K. Y., Kim, Y. G., Nam, I-S., Chung, J. S., and Lee, J. S., *Appl. Catal.* **75,** 267 (1991).
20. Sheffer, G. R., and King, T. S., *J. Catal.* **115,** 376 (1989).
21. Cormark, D., Poynter, D. A., Burlace, C. J., and Moss, R. L., *J. Catal.* **26,** 135 (1972).
22. Borgstedt, H. U., and Mathews, C. K., "Applied Chemistry of the Alkali Metals," p. 75. Plenum, New York, 1987.
23. Chuang, S. C., Goodwin, J. G., and Wender, I., *J. Catal.* **95,** 435 (1985).
24. Hotop, H., and Lineberger, W. C., *J. Phys. Chem. Ref. Data* **14,** 731 (1985).
25. Weast, R. C., (Ed.), "CRC Handbook of Chemistry and Physics," 1st student ed., p. D-35. CRC Press, Boca Raton, FL, 1987.
26. Yuh, S. J., and Wolf, E. E., *Fuel* **62,** 252 (1983).
27. Xie, Y., Gui, L., Zhang, Y., Zhao, B., Yang, N., Guo, Q., Duan, L., Huang, H., Cai, X., and Tang, T., *in* "Adsorption and Catalysis on Oxide Surfaces" (M. Che and G. C. Bond, Eds.), p. 139. Elsevier, Amsterdam, 1985.

28. Kennou, S., Ladas, S., and Papageorgopoulos, C. A., *Surf. Sci.* **152/153,** 1213 (1985).
29. Kennou, S., Ladas, S., and Papageorgopoulos, C. A., *Surf. Sci.* **164,** 290 (1985).
30. Dwyer, D. J., *in* "Physicians and Chemistry of Alkali Metal Adsorption" (H. P. Bonzel, A. M. Bradshaw and G. Ertl, Eds.), p. 307. Elsevier, Amsterdam, 1989.
31. Horwitz, C. P., and Shriver, D. F., *Adv. Organomet. Chem.* **23,** 219 (1984).
32. Norskov, J. K., Holloway, S., and Lang, N. D., *Surf. Sci.* **137,** 65 (1984).
33. Sachtler, W. M. H., Shriver, D. F., Hollenberg, W. B., and Lang, A. F., *J. Catal.* **92,** 429 (1985).
34. Hamilton, D. M., Jr., Willis, W. S., and Stucky, G. D., *J. Am. Chem. Soc.* **103,** 4255 (1981).
35. Collman, J. P., and Hegedus, L. S., "Principles and Applications of Organotransition Metal Chemistry," p. 259. University Science Books, Mill Valley, CA, 1980.
36. Butts, S. B., Holt, E. M., Strauss, S. H., Alcock, N. W., Stimson, R. E., and Shriver, D. F., *J. Am. Chem. Soc.* **101,** 5864 (1979).
37. Biloen, P., and Sachtler, W. M. H., *Adv. Catal.* **30,** 165 (1981).
38. Henrich-Olive, G., and Olive, S., *Angew. Chem.* **88,** 144 (1976).
39. Tacheuchi, A., and Katzer, J. R., *J. Phys. Chem.* **86,** 2438 (1982).
40. Papageorgopoulos, C. A., *Surf. Sci.* **75,** 17 (1978).
41. Michel, E. G., Oellig, E. M., Asensio, M. C., and Miranda, R., *Surf. Sci.* **189/190,** 245 (1987).
42. Oellig, E. M., Michel, E. G., Asensio, M. C., and Miranda, R., *Appl. Phys. Lett.* **50,** 1660 (1987).
43. Soukiassian, P., Bakshi, M. H., and Hurych, Z., *J. Appl. Phys.* **61,** 2679 (1987).
44. Karolewski, M. A., and Cavell, R. G., *Surf. Sci.* **219,** 261 (1989).
45. Phillips, J. C., *Phys. Rev. Lett.* **28,** 1196 (1972).
46. Bonzel, H. P., and Krebs, H. J., *Surf. Sci.* **109,** L527 (1981).
47. Campbell, C. T., and Goodman, D. W., *Surf. Sci.* **123,** 413 (1982).
48. Praliaud, H., Dalmon, J. A., Mirodatos, C., and Martin, G. A., *J. Catal.* **97,** 344 (1986).